Eur. Phys. J. H **43**, 523–549 (2018)
https://doi.org/10.1140/epjh/e2016-70064-9

THE EUROPEAN PHYSICAL JOURNAL H

The history of research into improved confinement regimes

F. Wagner[a]

Max Planck Institute for Plasma Physics, 85748 Garching bei München, Germany

Received 9 November 2016
Published online 5 January 2017

Abstract. Increasing the pressure by additional heating of magnetically confined plasmas had the consequence that turbulent processes became more violent and plasma confinement degraded. Since this experience from the early 1980ies, fusion research was dominated by the search for confinement regimes with improved properties. It was a gratifying experience that toroidally confined plasmas are able to self-organise in such a way that turbulence diminishes, resulting in a confinement with good prospects to reach the objectives of fusion R&D. The understanding of improved confinement regimes revolutionized the understanding of turbulent transport in high-temperature plasmas. In this paper the story of research into improved confinement regimes will be narrated starting with 1980.

1 Introduction

The release of energy from fusion processes between deuterons and tritons (DT-fusion) requires a high temperature to overcome the Coulomb potential wall, high density for frequent collisions and a high energy confinement time τ_E. For this purpose, fusion plasmas are confined by strong magnetic fields exerting the perpendicular Lorentz force. Plasma losses parallel to the magnetic field are avoided in toroidally closed magnetic geometry. The target parameters for the release of fusion power e.g. from a magnetically confined plasma are known quite from the beginning of this endeavour and are specified in Lawson's famous criterion [1]. The critical parameter combination, which results from a power balance consideration, is the fusion triple product $n_i T_i \tau_E$, with n_i and T_i the ion density and temperature, respectively. T_i has to be increased by an external heating system to about 20 keV to meet the maximum of the DT-fusion reaction rate; the density of the two plasma constituents – electrons and ions – has to be in the order of 10^{20} m^{-3}. The triple product governs the ratio of fusion power P_{fus} to loss power P_{loss}. For break-even[1], $n_i T_i \tau_E \sim 8 \times 10^{20}$ m^{-3} keV s; for ignition, it is $\sim 4 \times 10^{21}$ m^{-3} keV s. This quality has not yet been achieved today.

[a] e-mail: fritz.wagner@ipp.mpg.de

[1] Break-even implies that the ratio Q of fusion power to external heating power to maintain this state is one.

The triple product illustrates the important role of τ_E. It corresponds to the time, the plasma energy E has to be replaced because of transport losses: $dE/dt = -E/\tau_E + P_{heating}$ (1). Under steady-state conditions, the heating power $P_{heating}$ contributed by an external heating system and the internal α-particle heating resulting from the fusion processes themselves compensates the losses: $P_{loss} = E/\tau_E$. With a high confinement time, the T_i goal can be met with less heating power. Also the plasma density requires less external particle fuelling if the particle confinement time τ_p, defined in an equivalent form to equation (1), is long. It is an empirical indication that the transport mechanisms inherent to toroidal systems are such that τ_p and τ_E are linked and generally vary together. Because of the importance of τ_E, there is a systematic effort in magnetic confinement research to improve energy confinement. The reactor requires a τ_E-value of a few seconds.

Toroidal systems require two perpendicular magnetic field components to ensure stability and confinement, the toroidal field B_φ and the poloidal field B_θ. The resulting helical magnetic field lines map out closed nested toroidal flux surfaces which represent the essential structure of magnetic confinement. In the plasma core the innermost flux surface degenerates to the magnetic axis; the plasma edge is defined by the outermost flux surface.

The tokamak is the most advanced toroidal confinement system. The poloidal field is self-generated by a strong current flowing around the plasma ring. The other successful toroidal system, the stellarator, defines the two major field components from the outside by appropriately shaped coils. One advantage of the tokamak is that the plasma current provides already the ohmic heating power. Stellarators need external heating for proper operation.

The geometry of a toroidal plasma is foremost defined by the major radius R and the minor radius a. The strategy in fusion R&D is to increase the device size in steps incorporating the knowledge gained by the previous generation of smaller devices. τ_E grows with plasma size because a central temperature target can more easily be achieved with central heating at lower gradients. Within technical limits a higher τ_E allows a smaller and more cost-effective device.

In the 80ies, the world-wide largest tokamak, JET of the EU fusion programme, and the largest tokamak of the US fusion programme, TFTR, went into operation shortly followed by JT-60, the largest tokamak of the Japanese programme [1]. An important innovative concept was to define the outermost flux surface by a null in the poloidal field and a magnetic separatrix allowing divertor operation for plasma exhaust [1]. With a separatrix, the material limiter, whose inner edge defines the toroidal plasma cross-section and whose presence gives rise to impurity release and plasma recycling can be avoided. The first poloidal field divertors with up-down X-points were PDX in PPPL Princeton, staring 1978 and ASDEX in IPP Garching, starting two years later. Divertor operation turned out to be so successful that even JET, originally conceived with limiter, was converted to a divertor in 1994. ITER [2], the first experimental fusion reactor is, of course, a divertor tokamak.

Another, very important move at the beginning of the 80ies was the successful development and large-scale implementation of auxiliary heating systems. High heating power, more than an order above the ohmic level, pushed the high pressure plasmas to non-equilibrium states with unexpected properties. It was a gratifying experience that the self-organisation of plasmas under these circumstances carried the parameters closer to the ignition conditions and not unavoidably away from them.

The availability of high-power external heating systems in the 80ies represented an important advance also for helical devices. Up to then stellarators were heated ohmically. In this case, the unavoidable plasma current added internal rotational

transform[2] and changed the magnetic setting. Without ohmic current the confinement time improved in stellarators so that the authors could talk about "improvement of energy confinement" [3].

These advancements are the reasons why I start narrating the history of research into improved confinement regimes from about 1980 on[3].

2 Confinement physics of toroidal systems

In a plasma, electrons interact with each other by Coulomb collisions; the same happens within the ions and in non-symmetric collisions within the two species. These collisions cause radial transport with a rate determined by mean-free path and Coulomb collision frequency ν. In a magnetic field the plasma species gyrate around the force line limiting their excursions to the Larmor radii ρ_{L}. ρ_{L} adopts the role of the mean free path reducing the radial transport rate by a factor of $\sim 10^{15}$. This factor makes magnetic confinement a viable concept. The ion Larmor radius is larger than the electron one. Transport and confinement are expected to be governed by ion transport. This single particle view describes collisional transport under the classical conditions of a homogeneous field.

In toroidal geometry the field is inhomogeneous. The field, modified by the toroidal inhomogeneity ε_{t}, is represented in the simplest form by $\mathrm{B} = \mathrm{B}_{\phi}\,(1 - \varepsilon_{\mathrm{t}} \cos\theta)$. The field gradient, perpendicular to B_{ϕ}, causes superimposed particle drifts which lead to larger deviations of the particle orbits from the force lines. Under the axi-symmetric conditions of the tokamak field, the orbit deviations remain finite, however, but the transport rate increases and confinement is reduced. Because of the field inhomogeneity, the mirror effect[4] comes into play when particles move from the low-field side at the outside toward the high-field side at the inside of a flux surface. Particles with a low parallel velocity can be stopped and reflected. In this case, the drift effects are less compensated so that the excursions of the "trapped" particles are even larger than those of the "free" particles. The ions on trapped orbits govern τ_{E}.

Stellarators have unavoidably a 3-dimensional flux surface geometry. This fact alters strongly collisional transport because a further term adds to the magnetic field: $\mathrm{B} = \mathrm{B}_{\phi}\ (1 - \varepsilon_{\mathrm{t}} \cos\theta - \varepsilon_{\mathrm{H}} \sin(n\phi - m\theta))$. n and m describe the helical geometry of the field, ε_{H} the helical inhomogeneity. In stellarators, there is therefore a third class of particles which are locally trapped within the helical field well occupying a loss cone in phase space. These particles drift out of the confining volume and are lost. Because of the higher mobility of electrons the confinement time of stellarators is expected to be determined by electron losses.

At the beginning of the 80ies, a well-developed theory for collisional transport in toroidal geometry, the neo-classical[5] transport theory, existed for tokamaks both for heat, particle and impurity transport [4] and for stellarators for heat and particle transport [5]. Collisional transport should dominate quiescent plasmas representing

[2] A measure of the pitch of the helical magnetic field line moving around the torus.

[3] This paper is written for a general readership. Therefore, references are limited to primary publications and review papers. An extended version of this paper is available as IPP report (IPP 18-5, 2016) for interested readers from the field. This report contains an extensive list of references.

[4] Like in the magnetosphere of the Earth close to the poles

[5] Classical transport in magnetised plasmas denotes the cross-field transport due to Coulomb-collisions between charged particles; neo-classical transport applies to toroidal systems and includes the complex particle orbits and drifts occurring in an inhomogeneous field.

the lowest dissipation level. Unlike the tokamak, where the losses decrease with collision frequency ν toward the long-mean-free path regime of a reactor-grade plasma ($\Gamma \sim \nu$) they increase in helical systems: $\Gamma \sim 1/\nu$. In this case, scattering is beneficial because particles have a chance to leave the loss cone. Whereas the increase of τ_{E} is highly desirable in case of tokamaks, it is a necessity for stellarators. Without this measure, the stellarator concept is not a reactor option.

Up to now, we have seen the electron and ion species as independent, only coupled via Coulomb collisions. τ_{E} is determined by ion losses in the axi-symmetric tokamak and by electron-losses in the 3-dimensional stellarator. For transport equilibrium, electron and ion fluxes have to be identical, however. This is enforced by the radial ambipolar electric field $\mathrm{E_r^{amb}}$ which ensures charge balance $\Gamma_{\mathrm{e}} = \Gamma_{\mathrm{i}}$ in steady-state. The orientation of this self-induced field is such that the escaping particle is slowed down and the slower one is accelerated. Thanks to symmetry, $\Gamma_{\mathrm{e}} = \Gamma_{\mathrm{i}}$ is fulfilled in tokamaks independent of $\mathrm{E_r^{amb}}$. Tokamaks are "intrinsically" ambipolar. In case of stellarators, the electron and ion fluxes are not intrinsically ambipolar. $\mathrm{E_r^{amb}}$ represents a thermal force and affects strongly the neo-classical transport coefficients. The neo-classical transport equations for stellarators are therefore non-linear allowing several roots[6] – the electron root at low collisionality and the ion root at higher collisionality governing e.g. collisional transport at the edge. Several roots can appear simultaneously, leading to bifurcations in the neo-classical fluxes. Because of its explicit role the radial electric field and bifurcating transport equilibria were in the focus of stellarator researchers much before these terms started to play a role in turbulent tokamak transport. In tokamaks, however, $\mathrm{E_r}$ was found to tame plasma turbulence. This discovery and the gradual recognition that part of the underlying mechanism is a universal hydrodynamic process cover the major part of this paper.

Radial plasma transport is generally not laminar. Electron transport is far above the neo-classical level; ion heat conduction close to the neo-classical level is encountered only in specific corners of the operational domain. The radial transport of both plasma constituents is enhanced by plasma turbulence affecting heat, particle and momentum. One has to discriminate global magnetic instabilities like the $n = 1$, $m = 1$[7] mode in the plasma core which triggers periodic sawtooth relaxations[8] and may even dominate core transport from small-scale, broad-band turbulence in the form of electrostatic and magnetic instabilities. These instabilities are driven to their saturated states by the constituents of the pressure or parallel current density gradient, the dynamics of trapped particles and by unfavourable magnetic curvature. The universal dynamics is drift-wave turbulence where correlated pressure and electric field fluctuations lead to $\mathrm{E} \times \mathrm{B}$ flows perpendicular to the flux surfaces. The distinctive characteristics of the turbulence and its level depend on plasma parameters like the gradient lengths L_n and $\mathrm{L_T}$ of density and temperature, the temperature ratio $\mathrm{T_i/T_e}$, the magnetic shear S[9], the collision frequency (resistivity), the ratio $\eta = \vartheta_{\mathrm{r}} \ln \mathrm{T}/\vartheta_{\mathrm{r}} \ln n = L_{\mathrm{n}}/\mathrm{L_T} \ldots$ The most relevant drift-type fluctuations are the longer-wavelength[10] ion-temperature driven instability (ITG driven instability or η_{i}-mode) affecting in particular ion transport, the trapped electron mode (TEM) destabilised by a higher fraction of trapped electrons and the shorter wavelength,

[6] A "root" is the solution of an equation, the value of the variable for which the equation is zero.

[7] n, m describe the toroidal and poloidal topology of an Eigenmode.

[8] A local $n = 1$, $m = 1$ kink mode grows in time causing a periodic relaxation which repetitively flattens temperatures and densities in the plasma core.

[9] S is a measure of the radial variation of the magnetic field line pitch, the rotational transform.

[10] $k < 2\pi\rho_{\mathrm{L}}$, ρ_{L} being the ion Larmor radius.

higher mode-number electron-temperature-gradient instability (ETG driven instability or η_e-mode) which enhance predominantly electron transport. The saturated stage of these instabilities establishes the turbulent transport level. The dominant feature of these instabilities is that the induced transport rates steeply rise beyond a critical gradient. As a consequence of this threshold behaviour the relative temperature gradient is fixed close to critical values with the corollary that temperature profiles are rather stiff (this feature was called "principle of profile consistency" [6]).These canonical profiles are shape-invariant to the location of the heat deposition profile. Under these conditions, the edge transport plays a significant role with a strong impact on global confinement. In case of stellarators canonical profiles for T_e and T_i are not the typically case.

3 Confinement and transport studies in the early 80ies [7, 8]

At the end of the 70ties, a major breakthrough in plasma confinement happened giving fusion research a good start into the 80ies. At PLT, the then leading tokamak in Princeton, high T_i values beyond 5 keV were achieved with neutral beam injection (NBI) [1]. These results demonstrated that the ITG-modes were not as deleterious as anticipated. When these results were reported at the IAEA conference 1978 in Washington, Kadomtsev, then the lead-theoretician from the other leading fusion institution, the Kurchatov Institute in Moscow, congratulated after the presentation: "I congratulate you (R. Goldston) and the Princeton team on the very impressive achievement of reaching high ion temperatures and penetrating far into the collisionless region – a very important achievement for future reactor applications".

Unfortunately, this good spirit did not last very long. Three urgently awaited and originally welcome advancements in tokamak operation let to disappointments regarding plasma confinement. Under ohmic conditions τ_E increased linearly with density and, following the relation $\chi_e = a^2/4\tau_E$, the electron heat diffusivity χ_e decreased with it. This dependence, called Alcator scaling, was very favourable because the fusion triple product could have been expected to vary with density square.

Better wall conditions, the first advancement, allowed all devices to expand their operation toward higher densities. The density scaling did not continue, however, and the Alcator scaling quality was lost and τ_E even decreased approaching the density limit [1]. Later, this branch of the ohmic τ_E-scaling was dubbed "saturated ohmic confinement" (SOC) expanding the low-density LOC ("linear ohmic confinement") branch toward higher densities. Transport analysis showed that the ion transport increased in the SOC regime beyond the neo-classical level and that ITG turbulence was the dominant culprit for confinement saturation.

The transition to auxiliary heating, the second advancement, caused τ_E to severely decrease from the ohmic reference level. Plasmas entered the low-confinement L-mode which was stubbornly robust and reproducible. Again, enhanced ITG turbulence was made responsible for most of the L-mode confinement degradation. In the discussion phase of the 11th IAEA conference, H. Rebut, then director of JET, was cited talking about a "lack of significance of auxiliary heating" [9]. This gloomy situation became crystal clear to the participants of the 1984-EPS plasma physics conference in Aachen, when Goldston from Princeton, the same speaker who was applauded in 1978 for the high T_i-values in PLT, presented a multi-machine statistical analysis of the confinement behaviour with heating power P: τ_E degraded $\sim P^{-0.5}$. With this dependence as confinement basis – the so called "Goldston Catastrophe"[11] – the increased technical challenges and economic restrictions would hardly allow the realisation of an attractive tokamak reactor [10].

[11] M. Bell, PPPL Experimental Seminar, May 23, 2014.

The helical systems were luckier with the transition from ohmic heating to external heating and simultaneously to net current-free operation – representing now the proper way of stellarator operation: a distinct improvement of confinement was observed. But in 1986 Heliotron-E reported the degradation of confinement with heating power acknowledging that the ubiquitous L-mode with its infamous scaling has spread also to stellarators.

The final surprise come when the new large tokamak devices allowed to compare their τ_E – values with those of the smaller ones leading to an unexpected size scaling with little or even no scaling with minor radius a rather with an unexpected positive sensitivity on major radius R. The strong R-dependence pointed toward the role of toroidicity in the form of trapped particles or magnetic shear S.

There are operational ways to improve confinement as we have seen by increasing the density in stellarators or in ohmically heated tokamak plasmas, or the tokamak current in case of auxiliary heating. The primary interest of this report are cases, however, where a new confinement regime develops spontaneously as a bifurcation being the result of a process of self-organisation. The most prominent and relevant example of a spontaneous transition is the one from the low-confinement L- to the high-confinement H-mode whose "discovery" will be narrated further below in some detail.

4 Improved confinement with peaked density profiles [7]

Already in 1979, two regimes with different density profile shapes were observed in Pulsator tokamak [11]. The one with peaked profiles developed after the gas-puff had been reduced. It showed lower ion transport at the neo-classical level [12] and impurities accumulated in the plasma core as expected. In the case with broad n_e-profiles, the ion heat diffusivity was distinctively higher and no specific impurity effects appeared.

The same trick was used on ASDEX in 1988: A sudden reduction of the gas input led to the regime of improved ohmic confinement (IOC) [13]. The density profile peaked and the ion energy confinement improved. The reduction of the gas input seemed to be the pre-requisite to access this state. The instantly improved particle confinement maintained the particle content at a reduced fuelling rate. τ_E followed the linear low-density LOC scaling establishing the IOC confinement branch in the density range of the SOC regime but with superior values.

In CHS heliotron[12], the termination of the external gas puff led also to a peaking of the density profile and a concomitant improvement in the energy content at constant beam power. This behaviour, observed also in other helical systems, was called "reheat phenomenon" [14]. The confinement improvement also occurred in the density range where τ_E normally saturated following the linear variation at lower density.

The introduction of impurities e.g. neon injection into ISX-B plasmas let to a peaking of the density and ion temperature profiles and to an increase of confinement time by a factor of 1.8 above the standard level. This scenario, communicated in 1984 [15], could be realised in ohmic and beam heated plasmas. Besides the confinement improvement the linear scaling of τ_E with density was recovered. Similar results were reported from T-10, the largest tokamak of the Russian fusion programme, developing a radiative confinement mode, called B-mode with peaked density profiles in comparison to its low-confinement counterpart, the S-mode [16], with broad ones.

Of higher programmatic relevance were the auxiliary heated cases with peaked density profiles. In 1986, the discovery of the so called Supershot regime was reported by TFTR [17]. Later, the Supershot was categorized as a hot-ion (high-T_i) mode with a strong non-thermal ion distribution in the core, first developed at PLT as reported

[12] Heliotrons, an alternative to the stellarator also belong to the helical confinement family.

above. The Supershot "pioneered by Jim Strachan based on experience in PLT"[13] developed under strong core beam heating and low recycling edge conditions under balanced injection. Precondition of the Supershot regime was an extensive wall conditioning and preferentially the injection of lithium pellets into the low-density ohmic target plasma.

Under low recycling conditions the edge density was kept low and density and temperature profiles showed a strong peaking with the reward that τ_E increased above the corresponding L-mode level by up to a factor of ultimately 3.7. Core ion temperatures of up to 38 keV were achieved. The DT programme of TFTR was carried out in the Supershot regime and a fusion power of 6.2 MW could be achieved with 29.5 MW external heating.

Hot-ion modes were realised later in many other devices and confinement regimes. This mode was also developed in Heliotron-E in 1995 with strong beam heating and low wall recycling. The core ion temperature doubled and the confinement time increased by 30–40%.

Neutral beam injection opposite to the plasma current (counter NBI) into ASDEX plasmas led to a different confinement regime in the L-mode power range characterised by peaked density and ion temperature profiles [13]. The counter (ctr)-NBI regime was observed the first time in ASDEX in 1988. Like in other cases with peaked profiles a pre-requisite for the formation of this regime was the reduction of external gas puffing. With this initiation, the density profile gradually peaked and τ_E improved along with it.

The ASDEX results have been reproduced by JFT-2M, the JAERI tokamak, in 1992 confirming the striking difference in density profile shape between co- and ctr-NBI. The energy confinement improved by about 30%. DIII-D reported in 1996 a reduction of the turbulence level with ctr-NBI compared to co-injection. But the ctr-NBI regime had no wider resonance in the community possibly because impurities accumulated strongly. As the impurity result was not unexpected and in agreement with collisional transport theory no specific potential was seen in it. However, in 2002 ctr-NBI was picked up again by DIII-D and led to the improved QH-mode regime (see Chap. 5.3).

In 1994 the Textor team reported on the development of the "radiative improved (RI)-mode" which recovered the LOC density scaling but with auxiliary heating [18]. The RI-mode could be accessed by puffing small amounts of neon into the limiter discharge or unintentionally by Si erosion from freshly siliconized plasma walls. The most obvious feature of the RI-mode is again the peaking of the density profile. The confinement time reached very high values even close to the Greenwald density limit[14]. Because of the similarity in major characteristics and transport properties, the authors of [19] spoke about the "LOC-IOC-RI mode regime".

Transport analysis of plasmas with peaked density profiles evoked a convective particle inward flow to explain the density gradients in a largely source free zone. The dissipative trapped electron (DTE) mode is able to give rise to an inward convection transporting plasma from the source region at the plasma edge to the core. At peaked density profiles, turbulent ion transport (ITG instabilities) is reduced and the ion heat diffusivity drops to the collisional level. The increased impurity content of the plasmas e.g. by impurity puffing was found to be instrumental to reduce the ITG growth rate.

The peaking of the density profile could also be initiated by placing the particle source into the core region. In 1984, the Alcator C team was one of the first to report

[13] See footnote 9.

[14] The Greenwald density limit represents the operational limit of tokamaks toward high density. The limit manifests itself by a current disruption [1].

on confinement improvement by core particle fuelling via pellet injection [20]. Pellets are small frozen hydrogen spheres injected into the plasma with high velocity establishing a particle source in the plasma core. The low density LOC-regime was found to continue toward higher densities defining a third branch, the P-mode with improved confinement coalescing with the IOC-regime. Modelling showed that also in this driven case the turbulent ion transport dropped from the enhanced SOC level down to the collisional neo-classical limit. Core fuelling of ohmic and auxiliary heated plasmas became a standard technique on many tokamaks. On JET, regimes with improved confinement via density profile peaking by pellet injection were called PEP-mode, pellet-enhanced-performance mode [21].

The initial findings – reduction of ion transport, increase of core ion temperature correlated with a peaking of the density profile – were unanimously confirmed also by helical systems. Pellet injection into beam heated Heliotron-E plasmas caused density and ion temperature profiles to peak, $T_i(0)$ went up by about 50% and τ_E increased by 30–40% [22].

5 Improved edge confinement

5.1 The H-mode of ASDEX [23–25]

The "high confinement" H-mode [26] was discovered in ASDEX in February 1982 during neutral beam heating. The H-mode turned out to be a robust and ubiquitous confinement regime allowing finally the highest Q-values attained so far with JET. The beam phase of ASDEX discharge #4734 – the first H-mode - started as usual with an L-phase, the low-confinement counterpart, with degraded particle and energy confinement. But suddenly at constant power and without interference from the outside the plasma jumped into a new regime where both particle and energy confinement improved. The time for transition was much shorter than the energy confinement time and could be as short as $\sim$100 μs. This discrepancy in time scales pointed right away toward a bifurcating process.

The sudden transition into the H-mode could not be missed because it affected basically all diagnostics on ASDEX at the time: The signal of the D_α detectors monitoring the divertor or the main plasma dropped instantly at the transition. This became the dominant regime monitor. Simultaneously, the density increased in all interferometer channels. The two together clearly showed that the particle confinement improved. Diamagnetic and equilibrium β increased by an increment which was typically twice the one achieved by heating an L-mode. Despite of the density increase, also the electron temperature increased and the loop voltage dropped. Figure 1 is taken from the first publication on the H-mode [27]. The densities are compared of an L-mode (#4803) and the consecutive H-mode (#4804) discharge reflecting the bifurcation in particle confinement.

A critical condition had to be met for the H-transition manifested by a power threshold well above the ohmic power level of ASDEX. The neutral beam power had just been upgraded from 1.2 MW to 3 MW. This critical condition could be met with deuterium target plasmas at lower power than hydrogen plasmas. The mysterious isotope effect of confinement gained new weight by the mass-scaling of the H-mode power threshold. The inherently non-linear relation between energy content and heating power, which is the essence of this self-organised process, manifested itself by a cyclic process. The H-mode started with a dwell time on the low L-mode branch prior to the transition. The dwell time to the H-mode could be reduced in low-q operation. Larger sawteeth at an extended $q = 1$ radius were able to trigger an H-mode transition. After the jump onto the H-mode branch the plasma moved deeper into this regime.

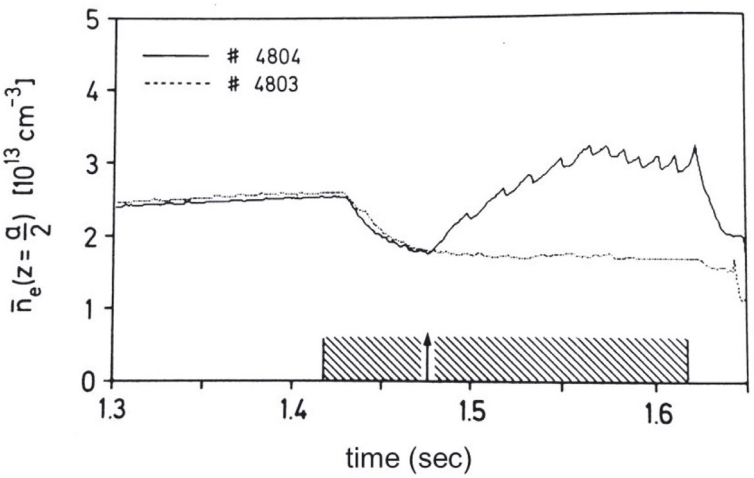

Fig. 1. Density variation during neutral beam injection for an L- and an H-mode plasma of ASDEX. The viewing line of the interferometer impacts at $r = a/2$.

When the beam power was finally switched off the plasma stayed in the H-phase again for a dwell time before it jumped back onto the L-mode branch. Generally, a hysteresis is observed in this cyclic process in the sense that the power threshold P_{thr} is higher than the power across the separatrix at the H-L back transition. The hysteresis concerns the nature of the bifurcation [28], the details depend, however, on many aspects which are not yet completely sorted out. With the power threshold, the sawtooth trigger and the dwell times it was clear that either the electron or the ion temperature must play a decisive role for the H-transition. They are the parameters, primarily affected by the heating power or by the thermal wave of a sawtooth. Maybe, because the edge electron temperature could be measured more easily and reliably than the edge ion temperature, many observations were made which supported T_e as crucial parameter. The successor of ASDEX[15], ASDEX Upgrade, could not confirm this conjecture. Decades later, Ryter et al. stressed "... that the ion heat flux is a key parameter in the L-H transition physics mechanism... The electron channel does not play any role". This is the generally accepted view now [29].

The sawtooth which triggered the H-mode was often the last one to appear and the plasma core was quiet during the H-phase. However, a new relaxation appeared at the edge. Edge Localised Modes (ELMs) [30] appeared right after the transition causing periodic losses. The large power fluxes during the ELMs are still a severe concern and a drawback of the H-mode. Since its discovery there has been a strong effort to explore ways to avoid ELMs without losing the good confinement (see Chap. 5.3). Those at ASDEX were not payed off. It was possible to suppress ELMs by carefully positioning the plasma inside the vessel and the energy confinement time benefitted from this endeavour. But so did also the impurity confinement. Without ELMs, the good particle confinement caused the impurity radiation to quickly increase. Only with ELMs a quasi-steady-state situation could be established.

[15] ASDEX stopped operation in summer 1991. The machine was dismantled by engineers and technicians from the Southwestern Institute of Physics (SWIP), transported to Chengdu, China, and set-up there in a brand-new building as HL-2A; the first discharge was in 2002. This device is still in operation and it has contributed and still contributes with many interesting results also to the understanding of the H-mode.

The H-mode and its characteristics as they could be identified with the limited diagnostic capabilities at the time were first presented to an international community at the 3rd Joint Grenoble-Varenna International Symposium, March 1982 [31] and then at the Baltimore IAEA conference in fall 1982 [32]. Outside the official agenda of this conference a special evening session was organised by Rutherford where the author of this paper was cross-questioned by an audience which fulfilled the ground rule of science – to be sceptical. Thereafter, the H-mode as a new object in plasma physics was accepted.

PDX [33] reported the H-mode in 1984; prerequisites were the operation with a separatrix and a more tightly closed divertor to locally concentrate recycling. Doublet III followed shortly thereafter [34] confirming the lower power threshold in deuterium. In 1985, JET demonstrated that the H-mode could also be realised in the worldwide largest tokamak [35]. Then, JET was still a limiter device which could, however, be operated with an X-point inside the vessel however close to the wall thanks to its shaping coils. The late A. Tanga was the motor behind these studies. JET benefitted from the H-mode because later, when it operated in DT, the highest Q of 0.65 was attained in the H-mode. Q short of 1 was expected for JET when the project was approved whereas its objectives were defined on the basis of the Alcator confinement scaling. The JET goal was finally met, however along a totally different confinement route and physics basis.

In 1987, JFT-2M discovered the H-mode also in the limiter configuration needing, however, twice the standard heating power. In all these devices the transition was spontaneous. In 1991, TUMAN, the tokamak of the IOFFE Institute in St. Petersburg, induced the H-mode by a strong gas puff applied to the plasma edge.

Spherical tokamaks (STs) with low aspect ratio A promise easier access to the H-mode and all major STs indeed operate in it [16]. Already the pioneering device of this tokamak variant, START of CCFE in Culham, showed H-mode transitions [36, 37]. MAST, the large successor of START reported on the H-mode in 2001, NSTX the spherical tokamak of PPPL followed in 2002 and Globus-M, the one of the IOFFE Institute in St. Petersburg, in 2007. These H-modes show all secondary characteristics known from conventional aspect-ratio tokamaks including ELMs.

In 1992 the H-mode was even realised in W7-AS stellarator with boronised walls [38] following the above mentioned recipe and in CHS heliotron with NBI [39]. The H-mode was achieved in W7-AS both with electron cyclotron heating (ECH) [1] and NBI at iota $\sim$0.5 when the configuration was limited by a separatrix and the poloidal viscosity by magnetic pumping was low. The W7-AS H-mode showed all the features of tokamak H-modes. The power threshold turned out to be rather low but operationally, the density had to be matched to the heating power. The H-mode was realised in 2004 in LHD at low field, and in the same year and – of specific importance for the future stellarator programme – in the optimised and quasi-symmetric helical device, He-J. The TJ-II heliac followed in 2010 with NBI and Lithium-coated walls. In an induced fashion using biasing probes, H-1, a heliac in Australia achieved H-transition characteristics.

The H-mode could be realised in all major versions of helical confinement irrespective of the details of their magnetic configuration [40, 41]. The H-mode of helical systems demonstrates its ubiquitous nature. Major differences to tokamaks are the symptoms of the 3-dimensionality of the system like orbit losses due to the helical ripple, the explicit role of the electric field in transport, and the damping of toroidal rotation. The H-mode in tokamaks is realised in systems with strong positive magnetic shear, in W7-AS and in TJ-II in systems with low magnetic shear, and in the heliotrons CHS and LHD in systems with strong negative shear.

[16] Against expectation, the power threshold turned out to be higher, however.

5.2 Understanding of the H-mode [24, 42, 43]

The SX-ray diagnostics consisting of an array of viewing cords provided the best resolution at ASDEX and had the capability to follow the thermal pulses resulting from sawteeth in the core travelling across the separatrix into the SOL. After beams had been turned on e.g. in a low-q discharge, sawteeth generally slowed down but grew in amplitude in the L-phase. If an H-transition happened during this period – triggered by a sawtooth larger than any of its predecessors – the thermal wave stagnated at the separatrix and grew in amplitude but did not propagate into the SOL any longer unlike the sawteeth before the transition. At the H-transition the SOL parameters basically collapsed within a sub-ms time scale. This observation led to the notion of an edge transport barrier – a zone of improved confinement right at the plasma edge [44]. Magnetic measurements with pick-up probes at the plasma edge showed a strong reduction in turbulence level pointing to the possible cause for the lower edge transport. Plasma profiles developed edge pedestals which are a characteristic feature of the H-mode confinement. ELMs appeared as a consequence of the steep pressure gradient and high current density within the pedestal. The edge gradients are not stably limited by transport rather repetitively hit a critical stability limit causing ELMs [45, 46].

The initial view on the H-mode was that the ohmic confinement had been restored and the L-mode was a short-lived accident. But the discovery of the H-mode under ohmic conditions stopped such speculations. Burrell wrote in his 89 paper [47]: "At plasma currents between 2.0 and 2.5 MA, we have found that energy confinement time in H-mode can exceed the saturated Ohmic confinement time by more than a factor of two..." Hence, the H-mode is a confinement branch in its own right.

Facing the complexity of the H-transition – obvious from the parameter dependence of the power threshold or the recommendations on the "how to get it" recipe list – it was evident that the physics is rather involved and its understanding required the joint effort of experiment, theory, and modelling. The regular exchange between these communities was institutionalised in the H-mode workshop series which was initiated by the DIII-D team with the first meeting in 1987 in San Diego. The most recent H-mode workshop, the 15th of its series, was held in IPP, Garching, Oct. 2015.

The task of theory was and still is to identify the mechanism acting at the edge with the potential to reduce the level of turbulence with the consequence that confinement improves and to identify the critical parameters or conditions which initiate the transition. In principle, an instability causing the anomalous transport at the edge of an L-mode plasma could be stabilised by the gradual change of the edge plasma parameters driven by increased heating power up to a critical stability condition. Many experimental observations would indeed support such a scheme. Therefore, in the pioneering period of H-mode transition theory, mostly in the 90ies, drift-wave and magnetic instability forms were perused and attractive stability conditions were indeed identified based on the separatrix peculiarities – the divergence of q, the increase of shear, the location of X-points, the neighbourhood to open field lines in the SOL and others. It is not the place here to go into any physics details as specifically an excellent review on this topic – "A review of theories of the L-H transition" – exists [42] summarizing the status up to 2000.

An alternative possibility to considering isolated instabilities which are ultimately stabilised is the notion of a bifurcating transition – multi-valued solutions exist for the same equilibrium fluxes, one with high transport rates and low edge gradients and the opposite case – low transport and steep gradients [48]. At the transition, the plasma jumps from the low to the high confinement branch. The fast time scale of the transition and the observation of a hysteresis in the sequence of states – L-mode,

transition, the H to L back transition – point to a highly non-linear process underlying the bifurcation.

A parameter moved into the centre of tokamak research which up to then was not of much explicit relevance – the radial electric field [49]. At the IAEA conference in 1984, R.J. Taylor had the question after the talk of Keilhacker: "Now, if it is a radial barrier, is it related to the radial electric field?" At the time of the conference, the question could not be answered as no experimental evidence was available. It is not surprising that "stellarator people" like S.I. and K. Itoh and K.C. Shaing explored the ambipolarity conditions at the edge of tokamaks in more detail. In stellarators with 3-dimensional flux surface geometry, collisional transport depends explicitly on the radial electric field which acts as drive for the radial fluxes and determines the transport coefficients. Therefore, the role of the electric field has always been of interest in stellarator research and stellarator theory has demonstrated the existence of branches with different ambipolarity conditions – the electron and the ion root [50] – before CHS [51] and W7-AS [52] could verify this in the experiment.

As the radial electric field turned out to play a crucial role in the L-H transition both the momentum balance and, as the ion pressure gradient is involved, also the power balance equation enter. Both neo-classical properties and turbulent processes come into play. Many non-ambipolar conditions can be constructed at the plasma edge, which could have an effect. They have been summarized in [53] in the form of $\varepsilon_0\varepsilon_\perp/\mathrm{e}\ d\mathrm{E_r}/dt = \Sigma\ \mathrm{I}^{\mathrm{non-amb}}$. The currents on the right side can originate from ion losses into the plasma boundary or caused by forces like the neo-classical parallel and poloidal viscosity intrinsic to toroidal geometry with a strong non-linear dependence on plasma flow or turbulent ones like turbulent Reynolds stress, neutral collisions of electrons and ions or wave momentum losses across the separatrix – processes which enforce an ambipolar response.

S.-I. and K. Itoh were the first in 1988 [54] to explore the role of the electric field in the L-H transition. They considered the loss of trapped ions at the plasma edge. Connor and Wilson, theoreticians themselves, write in their review paper [42]: "Remarkably, changes in $\mathrm{E_r}$ at the transition were predicted theoretically (...) before they were observed experimentally; the observation of these has led to their inclusion in many later theories".

The theory by Shaing and Crume, published in 1989 [55] also considered – like Itohs' theory – banana ion losses from the edge plasma under low collisionality conditions. The spin-up of the edge poloidal flow due to a radial ion current is balanced by parallel viscosity. In this theory, however, the electric field should become more negative at the transition. Both theories – Itohs' and Shaing's – were consecutively presented at the 1988 IAEA conference one proposing an electron the other an ion root solution for edge ambipolarity. Shaing, the second speaker, ended his presentation by stating: "the experiment has to decide about the sign of the radial electric field".

The challenge of the H-mode – to measure sophisticated plasma parameters at the plasma edge – ultimately with a time resolution in the range of 100 μs or better and a spatial resolution in the mm range was specifically accepted by the DIII-D team. Since the beginning of the 90ies, DIII-D has contributed with significant experimental evidence, which helped theory to develop a deeper understanding of the L-H transition and the H-mode, ending in a complete paradigm change in the understanding of turbulent transport [56]. Initially, DIII-D contributed with the following crucial findings:

– The radial electric field, which is slightly positive in the core, slightly negative at the periphery and again positive in the SOL develops a deep negative well at the location of the transport barrier within 500 μs of the transition [57]. The electric field confines the ions. DIII-D established that the $\mathrm{E_r}$-field change introducing

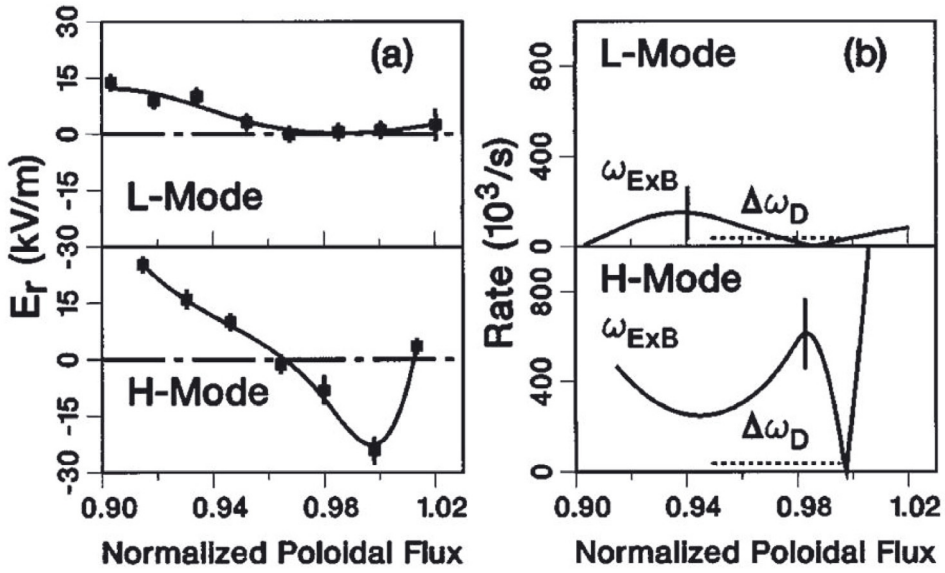

Fig. 2. (a) Plotted is the radial electric field in DIII-D shortly before and shortly after the L-H transition; (b) Compared are E × B shearing rate $\omega_{E\times B}$ with the turbulence decorrelation time $\gamma = \Delta\omega_D$ (see Eq. (2)) for the L- and H-mode phases shown in (a) (for details see [60], Fig. 5). (Reproduced from [60] with the permission of AIP Publishing. Doi:http://dx.doi.org/10.1063/1.873728)

strong E × B shear flow in the edge region is a fundamental property of the H-mode.

– The density fluctuations drop within the transport barrier by at least a factor of 2 within 100 μs of the transition identified precisely by the drop in D_α radiation [58]. This observation posed an enormous challenge to theory because the turbulence decreased in a region where the turbulence drive, the pressure gradient, forming the transport barrier, sharply increased.
– The particle flux, measured with Langmuir probes in ohmic discharges via the fluctuating constituents, density and E × B velocity, confirmed the indirect conclusions on improved global particle confinement [59] and were a direct proof of the impact of the drop in density fluctuations on radial flux and confinement.

The first radial electric field measurements were reported by R. Groebner at the 16th EPS conference on plasma physics in March 1989 in Venice and published in June 1990 [57]. At the L-H transition, the radial electric field, measured spectroscopically through the pressure gradient and the E × B flow of impurities via the Doppler shift of their lines, became more negative. Figure 2a compares the radial electric field in DIII-D shortly before and shortly after the L-H transition [60]. The development of a deep E_r-well at the plasma edge was later confirmed by all devices which studied this phenomenon. An independent and elegant technique to demonstrate the development of E_r at the plasma edge without resorting to poloidal flow measurements of impurities was develop at ASDEX Upgrade. The edge electric field affected the confinement of fast heating ions which happened to be trapped in the magnetic ripple of the discrete toroidal field coils during their slowing-down phase [61]. These ions are quickly lost by ∇B drift least an electric field improves their confinement. The rise of the energetic charge exchange flux at the H-transition and the delay time of this rise for more energetic ions could be used to demonstrate the drop of the radial electric field. The development of a deep E_r-field well at the very plasma edge starting

at the separatrix and extending a few cm into the plasma is the most conspicuous feature of the transport barrier.

In a key paper, which appeared in 1990 [62], Biglari, Diamond and Terry proposed a mechanism and a criterion for turbulence suppression which later, after general acceptance, was called the BDT criterion. The basic idea was that turbulent eddies causing L-mode transport are subject to poloidal flow at the edge. If this flow, actually the $E \times B$ flow as recognised right away, varies radially eddies are stretched and tilted and broken up to smaller and finally less transport relevant entities. More specifically, the fluctuations are decorrelated. A stabilising impact of sheared flows has already been pointed out by B. Lehnert in 1966 [63]. He wrote: "Thus, a non-uniform velocity should have a stabilizing tendency by "smearing out" the flute disturbance".

The BDT mechanism was first verified in TEXT ohmic discharges [64]. Within the natural $E \times B$ shear flow layer at the edge the turbulence correlation times and the fluctuation level were reduced whereas the density gradient was increased. DIII-D demonstrated the reduction of the radial correlation length of edge turbulence at the transition from the L- to the H-mode [60] confirming an important prediction of theory. The BDT criterion represents a quantitative relation for stability by sheared flow which is met when the shearing rate $\omega_{\mathrm{E\times B}}$ of the flow field is larger than the maximal linear growth rate $\gamma_{\max}$ of the least stable mode: $|\omega_{\mathrm{E\times B}}| > \gamma_{\max}$ (2); $\omega_{\mathrm{E\times B}} \sim \partial \mathrm{E_r}/\partial\psi$; the sign of the field variation is irrelevant. It was shown first by DIII-D [60] and later by many other devices that this condition was fulfilled within the edge transport barrier with strongly reduced turbulence level (see Fig. 2b). The shearing rate can be large enough to totally quench turbulence placing transport, generally ion transport, at the collisional limit. But intermediate states are possible where the shearing rate reduces turbulent transport without completely annihilating it.

The BDT model and criterion address only one important aspect of the H-mode – the mechanism for reducing edge turbulence via sheared flow. It does not provide the full understanding of the H-transition. The additional question is the origin of the radial electric field developing at the plasma edge in a spontaneous step. The simplest understanding would resort to the growing ion pressure gradient within the edge barrier which is a constituent of the radial force balance determining $\mathrm{E_r}$: $\mathrm{E_r} = \nabla \mathrm{p_i}/\mathrm{Z_i e n_i} - \mathrm{v_\theta B_\phi} + \mathrm{v_\phi B_\theta}$ (3). $\mathrm{E_r}$ becomes more negative with pressure gradient $\nabla \mathrm{p_i}$ and poloidal flow velocity $\mathrm{v_\theta}$ and more positive with toroidal velocity $\mathrm{v_\phi}$. All three constituents can introduce sheared flow. The initial flow and $\mathrm{E_r}$-field measurements of DIII-D showed a delay between the spin-up of poloidal impurity flow – the most striking flow feature – and the increase of the impurity edge ion temperature gradient [59]. The drop in $\mathrm{E_r}$ inside the separatrix coincided within 500 μs with the step of the $\mathrm{D_\alpha}$ radiation - the transition monitor. The ion temperature gradient as proxy for the ion pressure gradient followed along the slower confinement time. According to this observation, confirmed by others, the mean flow from the ion pressure gradient was not the primary cause for the transition.

The radial electric field deduced from the poloidal flow of impurities was found to be beyond the neo-classical level in DIII-D [57] necessitating an additional drive term in the poloidal momentum balance. It was conjectured that turbulent Reynolds stress (RS) could spin up transiently the poloidal flow beyond the neo-classical level [65] adding the so-called turbulence driven zonal flow (ZF) to the mean E × B flow of the ion pressure gradient[17] [66]. The turbulent RS is generated by the high level of turbulence in the L-phase as soon as the radial and poloidal velocity components $\tilde{v}_\mathrm{r}$ and $\tilde{v}_\theta$ develop coherence.

[17] The term "zonal flow" is borrowed from meteorology and oceanography denoting spatially restricted flow pattern e.g. zonal flows generated by baroclinic turbulence where sheared flow induces eddy tilting and Reynold stress is the mechanism to force zonal flows [66].

In toroidal geometry, the electric field component contributed by RS comes in the form of low-frequency flows, the zonal flows, or in the form of higher-frequency flows, so called Geodesic Acoustic Modes (GAMs) where compressibility is involved. ZFs and GAMs are radially localised space-charge perturbations with varying radial field direction and with $m = 0$ and $n = 0$ structure. Low-frequency zonal flows were first demonstrated by Coda in 2001 [67] and GAMs by Jakubowski [68] at the edge of DIII-D. Fujisawa proved their electrostatic nature and identified their geometry in the core of CHS heliotron using a dual heavy-ion-beam diagnostics [69]. The appearance of zonal flows in both forms of realisation demonstrated the non-linear coupling mechanism between small-scale turbulence and $E \times B$ flow. Both driven flow forms need turbulence drive as provided in the L-phase and they consequently disappear in the H-phase. A seminal review on zonal flows in fusion plasmas is written by Diamond et al. published in 2005 entitled "Zonal flows in plasma – a review" [70].

The experimental verification of the spontaneous self-regulating process of drift wave-type turbulence and ZFs via RS was an important contribution of smaller laboratory experiments to the understanding of the H-mode of the large fusion flagships. That RS can be a sizable effect in the momentum balance driving macroscopic flows was demonstrated in the linear device CSDX [71], in the Heliac H-1 [72], in the Torsatron TJ-IU [73] at CIEMAT in Madrid and with more detail in the same device operated later as TJ-K after having moved to Germany [74]. CHS showed how the combined effect of ZF and mean flow affects the high-frequency branch of the turbulence and identified the causality between flow and turbulence [75]. A complete documentation on sheared flows, their non-linear interaction with turbulence, the spectral flow of energy in this system and the consequences on confinement of H-1 Heliac plasmas was published by Shats et al. [76]. The role of this process for the H-mode transition was demonstrated by HT-6M tokamak in 2000 [77] and specifically its transiently increasing effectiveness just prior to the transition was shown in 2001 by DIII-D in [78]. On the background of all these data Burrell could conclude in his review paper on this topic [79]: "Considering all the experimental data, there is significant evidence that zonal flows exist in toroidal plasmas. In addition, there is evidence that both the low frequency zonal flows and GAMs can affect the higher frequency turbulence".

The efforts to understand the H-mode and the LH-transition have produced significant evidence for a new paradigm of turbulent transport. Confinement is not simply based on the transport caused by fully developed turbulence of regime-dependent instabilities but by a self-regulated state saturated by self-driven flows. In 2-dimensional turbulence where turbulent eddies can merge the spectral flow of energy is from smaller scales to larger ones (inverse cascade) till an $m = 0$, $n = 0$ potential structure of the size of the provided geometry, the ZF, is formed [80]. In this phase the turbulent eddies are strained-out – borrowing a technical term from 2-D turbulence in neutral fluids - and transfer effectively energy to the flow [72]. As this flow is sheared it eventually acts back onto the turbulence in a way the BDT criterion suggests. This intermediate step driven by RS reduces the turbulence level, improves the confinement, and allows steeper ion pressure gradients. The momentum balance plays a significant intermediate role in this stage. The increased ion pressure gradient or the concomitantly enhanced and sufficiently sheared mean $E \times B$ flow ensures that the BDT criterion is still met after the trigger period when E_r is now at the neo-classical level again [81]. Therefore, the final state is governed by the edge power balance. In total, a quiescent state of good confinement with high fusion reactor relevance has emerged in a self-organising manner from a state with a high degree of turbulence offering little perspective for the technical objectives of magnetic confinement research.

The chicken-and-egg question of causality [60] in the circular interplay between turbulence and flow may be obsolete because the object is the drift-wave-zonal flow

complex. Nevertheless, there are empirical recipes for attaining the H-mode and there is a clear driving agent, the heating power both pointing to a chain of actions: The larger the heating power is, the more probable is the transition and the shorter is the preceding L-phase.

The leading role of the radial electric field at the edge was demonstrated by triggering the H-mode or plasma states with edge transport barriers using biasing probes inserted into the plasma [82] or by biasing divertor target plates [83]. The first relevant experiments were carried out at CCT at UCLA [84], expanded in much detail by TEXTOR tokamak [85]. The theory of plasma biasing is provided in reference [86]. These experiments clearly demonstrated a phase lag between electric field, applied from the outside, and the reduction of the turbulence level and the increase of the edge pressure gradient. The agent is the electric field. JFT-2M confirmed this result by varying the power threshold with plasma biasing. When biasing added to the intrinsic E_r, P_{thr} decreased; biasing at opposite polarity increased it [87].

A more formal way to look at the L to H transition and the H to L back transition was from the point of view of bifurcation theory [53] considering specifically intermediate states (dubbed I-phases) where the plasma oscillates between the two equilibrium branches in the form of limit-cycle-oscillations (LCO) [88]. Transitions with extended I-phases could be cultivated experimentally by operating close to the power threshold and thanks to detailed edge measurements the causality between the various parameters involved could be elucidated in quite some detail. Formally, the bifurcation and the associated limit-cycle-oscillations could be described by a predator-prey equation system with the turbulence adopting the role of the prey feeding the sheared $E \times B$ flow which itself plays the role of predator finally killing it [89,90]. This Ansatz treats the combined flow and turbulence system self-consistently and identifies the phase shift between turbulence and flow in the form of zonal flows or of the equilibrium $E \times B$ flow and highlights their instrumental role for the transition [91]. In the L-phase, the flow is found to lag behind the turbulence – as expected. In course of the I-phase the LCO slow down. This reflects the fact that the role of the ion pressure gradient for the flow increases and the periods where the decorrelation time > inverse growth rate (Eq. (2)) are prolonged. The continuously increasing ion pressure ultimately stabilises the situation. After this prelude the mean background flow ensures the low turbulence edge state as long as power is put into the system. There are two predators – ZFs when the hunt starts and the mean flow, when the prey resigns. This sequence of affairs is presented in detail in [92] and confirmed by the results of many other devices [93].

The historical account of elucidating the physics of the H-mode comes to an end here. Doyle [94] of DIII-D concluded in 1992: "That the change in edge profiles is a consequence of the change in E_r, and not vice versa, has recently been shown by analysis of fast time resolution CER[18] data. (...) the increase in density and temperature gradients in the edge lag the changes in E_r, and thus cannot be the cause of the change in E_r." M. Cavedon, who reported at the 2015 H-mode workshop, writes in his recently submitted paper: "We have provided clear experimental evidence of the key role of the neo-classical flows in the L-H transition physics whereas no evident sign of zonal flows was observed at the H-mode onset. And Y. Andrew from JET goes a step further and reported in 2008 [95]: "These data[19] suggest that the development of significant shear in E_r arises as a consequence of the high confinement phase of the plasma and is not required to enter or maintain the H-mode on JET. This important result indicates that $E \times B$ shear suppression of turbulence does not trigger the transport barrier formation, although it may well play a role in transport

[18] CER = charge exchange recombination spectroscopy
[19] The ones presented in the paper.

barrier sustainment and dynamics." Obviously, like to Rome, different routes lead to the H-mode. More research is necessary here before the history book can finally be closed.

5.3 Improving the H-mode

All experimental teams try to further improve the H-mode confinement beyond the typical factor of two in τ_E above the L-mode. Several further improved confinement regimes came about surreptitiously while pursuing other priorities – e.g. starting additional heating early in the discharge during current ramp-up to economise on stored energy in the primary transformer – or developing high-β_p scenarios with large bootstrap current j_{bst} [1] for steady-state operation – or using impurity radiation to ameliorate exhaust conditions and to protect the inner wall. Another line of research dealt with the nuisance which unfortunately accompanies the H-mode, viz. edge localised modes, so called ELMs. In a repetitive relaxation process a large amount of energy ($\Delta W/W \sim 5$–10%) is released within a few 100 μs. The resulting power flux onto the divertor target plates is difficult for engineers to handle even with the best material and cooling technologies. There is a tremendous effort to avoid ELMs and the inherent instabilities by external means – resonant and non-resonant techniques using saddle coils, so called resonant magnetic perturbation coils with different toroidal and poloidal periodicities [1]. These coils demonstrated their efficiency in several experiments but this technique cannot yet guarantee their complete avoidance. But suppressing ELMs can be a double-edged matter. Without ELMs, the confinement may be too good for impurities and the plasma can get increasingly dirty. As the integration of such saddle coils into a fusion reactor, located close to the plasma surface, poses a technical challenge a much better way would be to discover and to develop scenarios without ELMs and, if possible, without having to accept impurity trade-offs. The plasma itself should do the job.

The VH (very high)-mode was realised in DIII-D in the early 90ies in configurations with improved edge stability by strongly shaping the plasma cross-section [96]. The VH-mode is generally without ELMs and has a confinement time a factor of up to 3.5 above the L-mode level. The most characteristic feature of the VH-mode is a broader edge transport barrier with the E_r-shear extending from the edge to $r/a \sim 0.6$ resulting in higher pedestal parameters (at gradients close to the stability limit). In the radial range closer to the core, it is the enhanced toroidal flow which contributes to the radial electric field shear.

In the effort to cope with the power exhaust conditions affected by ELMs, ASDEX Upgrade developed 1995 the so called "completely detached H-mode" (CDH) employing neon puffing [97]. Under conditions where the plasma stayed detached and a high power fraction was radiated off (up to 90%) the confinement did not degrade. Also the ELMs stayed small and their power was dissipated at high density. Later a significant improvement of confinement in N_2 seeded deuterium plasmas typically by 25% was noted [98]. The improved confinement was caused by an increase of the ion energy content but unlike the cases discussed above the improvement was not correlated with a peaking of the density profile. DIII-D repeated these experiments and observed a reduction of the ion transport also in the core of the plasma specifically an improvement of momentum transport. There is evidence that the improvement is due to $E \times B$ shear flow stabilisation within the core region.

Another variant, originally dubbed "Improved H-mode", was published by ASDEX Upgrade in 1999 [99]. The improvement came about by first enhancing the stability of the magnetic configuration with higher triangularity and by reorienting the NBI system to more off-axis deposition. While the H-mode edge was maintained in this

scenario the core confinement improved owing to a peaking of the pressure profile. The enhancement of the confinement was about a factor three above the L-mode level. The improved H-mode requires a subtle trade-off between current and pressure profile development so that the central q-value remains shortly above 1. The highest value of the fusion triple product in ASDEX Upgrade was realised in the "Improved H-mode". Two years after ASDEX Upgrade, DIII-D reproduced this confinement mode achieving bootstrap current fractions up to 50%.

The instabilities underlying ELMs are triggered by too steep a pressure gradient at the plasma edge. The remaining H-mode transport is too low to prevent hitting the stability limit so that the MHD stability limit is periodically violated each time causing an ELM and leading thus to a quasi-steady state situation. The strategy for suppressing ELMs and thereby improving the H-mode is clear - avoidance of too steep edge gradients. Several improved regimes without ELMs have been identified where the edge pressure gradient is clamped below the critical instability limit by a quasi- or weakly coherent mode residing at the very plasma edge with the beneficial trait to exclusively reduce particle transport leaving energy transport largely unaffected. This is an interesting but not yet well understood constellation.

C-Mod reported at the 1996 IAEA conference on the development of EDA, the "Enhanced-D_α H-mode" [100]. The denotation comes from the observation of enhanced D_α radiation from the inner SOL beyond the X-point. ELMs were replaced by a quasi-coherent (QC) mode residing at the plasma edge, which obviously limited both the edge pressure to below the ELM stability border and the particle confinement maintaining a clean plasma.

In 2002, DIII-D went public with an H-mode without ELMs and without sacrificing the confinement quality [101]. This mode was originally established with counter neutral beam injection when additionally strong pumping had been applied. Under these circumstances and with beam fuelling alone, ELMs were absent or rare and small so that the mode was dubbed quiescent H-mode (QH-mode). Because of the so-called edge harmonic oscillation EHO, residing in the gradient region at the plasma edge and driven by it, the particle confinement was low and the QH-mode could be maintained for long periods without the usual corollary of increasing density or impurity content. The energy confinement time did not seem to be affected by this oscillation. The presence of the EHO was found to be crucial.

In 2003, ASDEX Upgrade realised the QH-mode, JT-60 followed in 2004 and JET published results in 2005 confirming the major findings of DIII-D – ctr-NBI and recycling control with preparatory glow-discharge cleaning, strong pumping, and a careful positioning of the plasma inside the vessel, and, in case of JET, beryllium evaporation.

Another promising advanced mode of this kind may be the so called "improved L-mode", realised first on ASDEX Upgrade in 1994 [102] and later, 2010, rediscovered by Alcator-C-Mod and dubbed "I-mode"[20] (improved mode). The first publication of C-mod is entitled: "I-mode: an H-mode energy confinement regime with L-mode particle transport in the Alcator C-Mod" [103]. In a related paper by ASDEX Upgrade, the authors write: "Therefore, these plasmas exhibit an edge transport barrier for heat but L-mode particle transport" [29]. These two nearly identical statements highlight the most promising feature of the I-mode, the reduced particle transport remaining at the level of the L-mode.

The I-mode develops gradually rather in the form of a soft bifurcation. A temperature edge pedestal forms comparable to the one of the H-mode. The density profile at the edge does not change at the L–I transition. Therefore, the edge pressure gradient

[20] Not to be confused with the I-phase.

remains beneath the critical ELM limit of the H-mode. As a consequence, the E_r-field well deepens at the transition to the I-mode but not to the depth of the H-mode.

The important feature of the I-mode is a weakly coherent mode (honoured by the acronym WCM) acting at the edge where otherwise ELMs are located. As in the other cases, this mode seems to provide the mechanism which allows preferentially particles to escape circumventing the canonical link between energy and particle transport. The I-mode can exist in a large parameter range and is a candidate for an ITER operational scenario.

W7-AS reported in 2002 shortly before the device was de-commissioned also on a confinement regime without ELMs with H-mode energy and L-mode particle confinement [104]. This regime developed at high density. Most spectacular was the development out of a quiescent H-phase with strongly increased impurity radiation. Initiating a further density increase by gas puffing gave rise to a sudden self-purification of the plasma shortly before the discharge would have collapsed. In this very pure high-density phase, beyond the formal Greenwald density limit, the energy confinement surpassed the standard scaling value by a factor of two. The analysis of the impurity transport yielded a strong reduction of the inward convective flow. This was also manifested by the density profile which was dead-flat up to the separatrix. The critical density for the formation of the HDH-regime increases with heating power up to 2.2×10^{20} m^{-3} at 3 MW absorbed beam power. Under these conditions the divertor was partially detached and plasma exhaust was strongly eased. The physics of the HDH-mode could not be resolved in the remaining experimental time.

6 Internal transport barriers [105–107]

In another R&D line of fusion research – making the pulsed tokamak discharge steady-state – external current drive by directed energetic particles or e.m. waves [1] was employed to plasma scenarios displaying a high bootstrap current j_{bst}. The bootstrap current density is large at the location of the off-axis pressure gradients leading to broadened current density profiles. As j_{bst} rises with β_p confinement and stability governed by plasma shape, pressure- and q-profiles have to be considered together for these high-β/β_p scenarios. In order to maximally utilise the ohmic current drive for long pulse durations, or, in another scenario, to avoid the early onset of sawteeth in the plasma core, auxiliary heating had to be applied very early in the discharge. Such scenarios start with a broadened non-equilibrium current profile j(r) which can be even hollow when the ramp rate is higher than the current diffusion time prolonged by early electron heating. Under these circumstances a different set of equilibria develops where the q-profile does not rise monotonically to the edge but can form a minimum with magnetic shear $S = 0$ around mid-radius and even reversed magnetic shear toward the core. JET was one of the first to start with early heating in the current ramp-up phase to save magnetic flux in the primary system for longer plateau periods needed for pellet injection as reported by Schmidt 1988 at the IAEA conference in Nice [108].

For the necessary high bootstrap current confinement has to improve to yield steep pressure gradients at a plasma radius relevant for steady-state scenarios. There are several arguments in favour of stability and confinement improvement with low or even reversed magnetic shear [109]. In a well prepared discharge an "internal transport barrier" (ITB) – a radial zone with steep gradients – can develop spontaneously located about half-way to the edge. An ITB develops like its counterpart, the ETB, the external transport barrier of the H-mode, in a spontaneous step as a threshold process. The target plasma has to be carefully prepared – low recycling wall conditions and low ohmic starting density. The current ramp-up plays a crucial role to enter the plateau phase with a q-profile with either q(0) close to 1 and an extended low-shear

zone or, distinguished by an off-axis minimum, with weak negative shear ("reversed shear", RS) or strongly negative shear ("enhanced negative shear", ERS) in the core region. In such a case the core profiles of transport related parameters – density, temperature and rotation – can develop a base point at or close to the minimum in q where the transition threshold is lowest.

ITBs in the ion channel and in the density are obtained relatively "easy". The easiness is measured on the resilience of the electron transport to also form transport barriers [110]. ITBs in T_e, the electron temperature, (T_e-IBT) require specific settings for electron heating and current drive by ECH and electron cyclotron (ECCD) or lower hybrid current drive [1]. But for all three state parameters, a strong central source helps to form ITBs – strong ion heating as in the hot-ion mode or strong electron heating for T_e-ITBs [111] or pellet injection to peak the density profile like in the PEP-mode.

The term "internal transport barrier" was coined in the paper by Koide at al. from 1994 entitled "Internal transport barrier on $q = 3$ surface and poloidal plasma spin up in JT-60U high-β_p discharges" [112]. The new regimes have been dubbed "high-β_p mode" in JT-60U, "reversed shear" (RS) or "enhanced reversed shear" (ERS) mode – in TFTR [113] and finally "negative central shear" (NSC) mode in DIII-D [114]. The ERS mode excels by stronger negative shear than the RS mode reducing further particle and ion heat transport and even electron transport leading to a very low fluctuation level. Together with current drive high β_p scenarios with ITBs are qualified for steady-state operation. At JET, the term "OS mode" – optimised shear – is used for discharges with flat or reversed core q-profiles where the profile change is initiated by current drive prior to the main heating pulse [115]. In this mode, JET has carried out DT experiments and reached the highest fusion yield with deuterium plasmas. Another example is the lower hybrid enhanced performance (LHEP) regime of TORE SUPRA [116] characterised by a flat or even reversed q-profile in the core and larger magnetic shear in the gradient region. Figure 3 shows profiles with ITBs in density and temperatures and reversed shear in the plasma core of JT-60 U [117].

With an ITB, it is generally the ion pressure gradient which is strongly increased and the ion transport drops – in case of DIII-D to the neo-classical level, in case of TFTR even below it. This surprising aspect has been confirmed by JT-60U. The pressure gradient length compares with the banana width of thermal ions violating in these cases the ordering of standard neo-classical theory. Transport analysis showed that the expected effect of low or reversed magnetic shear on turbulent instabilities – to reduce growth rates and transport – does not fully explain the local transport improvement. The presence of a power threshold to develop an ITB, increasing with magnetic field like in case of ETBs, demonstrated already the existence of a further mechanism based on kinetic effects and not on equilibrium features. As for the H-mode and the ETB, also for ITBs, shear flow decorrelation plays a decisive role to reduce the turbulence level and to improve gradients in a radial range further in. The leading term in the E_r formation can be the pressure gradient whose signature identifies an ITB. Whereas toroidal flow does not play a major role in ETB formation (apart from the VH-mode) the v_ϕ-term in the radial force balance (Eq. (3)) can dominate under conditions of strong parallel beam heating. The v_ϕ-term in the force balance gives rise to a positive E_r-field with shear. The BDT-criterion (Eq. (2)) is, however, independent of the sign of the field shear. Also for ITBs like for ETBs a loop process is initiated mediated by the E_r-shear where turbulence is reduced and gradients are steepened.

The role of $E \times B$ shear flow on turbulence at the location of an ITB has been demonstrated in steps similar to those of the H-mode. The turbulence level is reduced within the ITB and the BDT criterion is fulfilled whereas the instability growth rate $\gamma^{\max}$ is reduced owing to low or negative shear. Also the radial correlation length of the turbulence is found to be reduced. Of special value is the recognition of the E_r-field

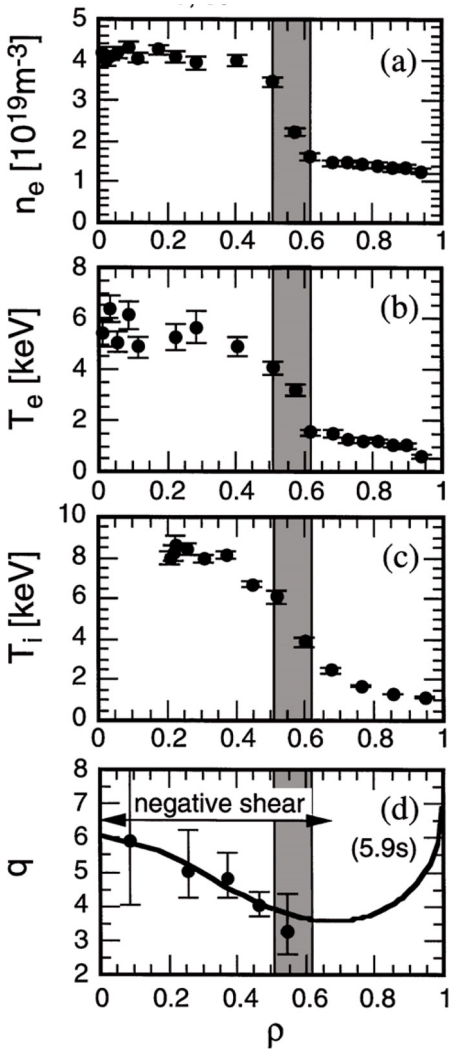

Fig. 3. Plotted are density and temperature profiles from JT-60 showing an ITB together with the q-profile demonstrating reversed shear in the core [117]. (Reprinted with permission of T. Fujita et al. [117], @1997 American Physical Society. Doi:https://doi.org/10.1103/PhysRevLett.78.2377)

shear in TFTR and in DIII-D. In both cases it is large but in case of TFTR [118] it is negative, as conventionally the case with steep ion pressure gradients, whereas in DIII-D it is positive because of a large $v_\phi B_\theta$ contribution to E_r (see Eq. (3)).

Discharges characterised by an ITB excel by a very high fusion yield and indeed the best values of this parameter were obtained in several devices with improved core confinement [40]. The highest $Q_{DT} \sim 1.05$ (extrapolated however from DD operation) has been achieved in JT-60U with reversed shear and an ITB [119].

Also helical systems have reached ITBs based on the quench of turbulent transport. In CHS, ECH let to an T_e-ITB in a radial zone with reduced turbulence level and a corresponding change in the E_r structure. Pellet injection into Heliotron-E let to strongly reduced ion heat transport and, thanks to profile peaking to a reduced negative electric field with strong shear. An interesting case has been observed in W7-AS

within the transition layer between the electron root in the core and the ion root further out [120]. Within 1–2 cm E_r drops by 40 keV/m. In this case the shearing rate in the transition zone exceeds the instability linear growth rate and an internal transport barrier develops. The development of the ITB shows dithers close to the transitional power and a hysteresis between creation at high and loss toward low power.

The two features, ETB and ITB, can be merged in the experiment [97] though ELMs can impede, even prevent the formation of ITBs and the ETB can weaken the flow shear in the plasma core. Nevertheless, the H-mode edges have been combined with the "high-β_p mode" [112], the "PEP mode" [121] and the "NCS mode" [122]. With regard to the two goals of ITER – $Q = 10$ in an inductive and $Q = 5$ in a steady-state scenarios, improved confinement will play a major role. In so-called hybrid scenarios, improved H-modes with ETBs are combined with an extended range of low magnetic shear and $q(0) \sim 1$ in the core [96]. They could help to reach the first goal. So called advanced tokamak (AT) operation with strongly improved confinement and stability may qualify for steady-state operation. T.S. Taylor proposed an AT with VH-mode edge and reversed shear core conditions with the core also being in the second stable regime [123]. This confinement and stability scenario has been called second stable core (SSC) – VH-mode – maybe the best fusion research can offer up to 2016.

7 The universal role of shear flow decorrelation [47]

A carefully MHD analysis of the JET PEP mode [124] – a representative of the peaked density profile confinement category – showed that also in this case the q-profile seems to be reversed. Specifically, the density gradient is very effective in flattening the q-profile. Within the development of the Supershot characteristics, the density gradually peaks and the ion temperature follows along in radial ranges where the electric field develops shear. The increasing shearing rate reduces ion transport causing the ion heat diffusivity to drop with increasing T_i [125]. The Supershot profiles bootstrap themselves toward a transport equilibrium with excellent core confinement. Toward the edge, the shearing rate loses its effectiveness and turbulence and L-mode transport prevail.

The density profile peaking with ctr-NBI (see Chap. 4) has been analysed in [126]. It is conjectured that the anomalous convective inward velocity stems from the poloidal friction force interacting with the fluctuating electric field. The transport analysis of the RI-mode, reproduced in DIII-D, stressed the role of $E \times B$ shear flow stabilisation of turbulence at reduced growth rate owing to the presence of impurities [127]. The other ohmic cases with peaked profiles have not been analysed in retrospect in much detail. Nevertheless, GAMs have also been observed in ohmic plasmas [128] and also their interaction with drift-wave turbulence has been documented [129]. Possibly, self-regulating mechanisms set the turbulent level also under these low β conditions.

In summary, the improvement of confinement seems to be based on one primary mechanism which applies to both ETBs and ITBs and plasmas with peaked density profiles, which is shear flow decorrelation of turbulence. For the BDT-criterion (Eq. (2)) to become effective, prerequisites seem to be necessary. They seem to differ for ETBs and ITBs. The proximity of the edge separating the electrostatic potential of open and closed field lines easing the development of non-ambipolar conditions affects specifically the left hand side of equation (2) allowing ETBs to form. The low or even reversed magnetic shear conditions in the plasma core (like the high T_i/T_e in the hot-ion mode, increased Z_{eff} in cases with impurity seeding or increased magnetic

edge shear) reduce the growth rate of instabilities and affect the right hand side of equation (2).

8 Conclusions

The preoccupation with enhanced confinement regimes created a new understanding of turbulent transport historically dubbed "anomalous transport" because its governing physics eluded rapid clarification. A credible conception has emerged now – gradient driven drift-wave type turbulence develops to a level stet by the spatial variation of neo-classical and self-driven plasma flows. Turbulence and flows have to be treated self-consistently. This frame of understanding has the additional beauty that one component is not exclusively restricted to plasma physics but rather unique and encountered also in other fields where sheared flows within neutral fluids regulate turbulence. Examples are flows within the planetary atmosphere e.g. leading to the rings of Jupiter and Saturn, flows in the sun's convection zone, the polar jet stream in Earth's atmosphere or oceanographic flows like the Gulf stream. Examples are collected and discussed in [130]. Diamond et al. write in their 1992 IAEA fusion energy conference paper [131]: "... mean shear amplification is an example of a type of self-organisation process known for a long time in geophysical fluid dynamics (...) and recently encountered in the plasma community...".

The other feature of the new confinement paradigm is rooted in one of the most basic plasma characteristics as plasmas are composed of light negative and heavy positive charges with strongly different mobilities – the law of ambi-polarity and the related electric field which ensures transport equilibrium within this medium. In magnetically confined plasmas the ambi-polar electric field causes sheared flows which interact with turbulence and regulate its level.

Some of the essential preconditions to improved confinement regimes are surprisingly identical for tokamaks and stellarators: recycling control and avoiding gas puffing, sufficient heating power to overcome thresholds and peaking of the density profile. ETBs and ITBs develop in both concepts with the addition of neo-classical ion- and electron root physics in helical systems. Recycling control rewards with good confinement when limiters, specifically low-field-side limiters are replaced by a separatrix, graphite first walls by metal ones and gas-puffing by pellet injection. Also the H-mode power threshold can strongly increase with excessive gas puffing or decrease when the edge source is moved into the divertor or to the high-field side. The degree of power degradation and the additional degradation toward the density limit suffer from gas puffing. It will be a challenge to maintain recycling control under steady-state conditions when walls are getting saturated. In the future programme, non-inductive scenarios with continuous pellet refuelling have to be cultivated. Gas puffing as the main particle source should be forbidden!

Building upon the accumulated knowledge, the design of ITER includes a strongly shaped cross-section with an X-point and a divertor and a low-recycling metal wall in agreement with general perception. Shaping will improve stability from which also the confinement will benefit after the formation of ETBs and ITBs. Thanks to the advanced confinement modes, ITER might go beyond its canonical goals of $Q = 10$ in the inductive and $Q = 5$ in the steady-state scenario. In the first case, hybrid scenarios might allow to push Q, in the second case the benefits of AT scenarios might help to reach or even to surpass the goals. But the advanced scenarios are subtle and tend to disruptions. Also ELM suppression, α-particle confinement in case of the high-β_p mode, impurity accumulation in cases with peaked density profiles, and, generally, electron transport need further consideration. At the end, ITER has to identify

the best confinement conditions by itself. But guidelines are available from the research done in the past.

Steady-state operation is the main objective of helical systems. The most advanced device, Wendelstein 7-X, has started operation when this report was written. The W7-X magnetic design promises good stability, a reversed shear configuration built into the vacuum field and the E_r-field effects of a 3-dimensional configuration. Regarding transport, W7-X is optimised guided by neo-classical physics; the overall optimisation results in features which, as we have seen, promise access to confinement regimes with reduced turbulence.

B. Kadomtsev and O.P. Pogutse stated in 1970 [132]: "The question of achieving controlled fusion thus reduces to the possibility of reducing the turbulent diffusion coefficient to a value that is two orders of magnitude smaller than the Bohm value"[21]. Maybe, the conclusion of this paper could be – yes, mission successfully completed. In the radial zones of ETBs and ITBs, turbulent confinement has been strongly reduced, the ion transport can be at the neo-classical level for all radii [120] and the local confinement is effectively governed by the stability of global modes at gradients which could even violate the assumptions of conventional neo-classical transport theory. Hardly more could have been asked for.

Open access funding provided by Max Planck Society.

References

1. Introductory textbook into fusion: *Fusion Physics*, edited by M. Kikuchi, K. Lackner, M.Q. Tran (IAEA, Vienna, 2012).
2. ITER Physics Basis, Nuclear Fusion **39**, 2137 (1999).
3. WVII-A Team and NI-group, in *Proc. 9th Int. Conf. on Plasma Physics and Controlled Nuclear Fusion Research, Baltimore, 1982* (IAEA, Vienna 1983) Vol. 2, p. 241.
4. F.L. Hinton, R.C. Hazeltine, Rev. Mod. Phys. **48**, 239 (1976).
5. A.A. Galeev, R.Z. Sagdeev, Rev. Plasma Phys. **7**, 257 (1979).
6. B. Coppi, Commun. Plasma Phys. Control. Fusion **5**, 261 (1980).
7. F. Wagner, U. Stroth, Plasma Phys. Control. Fusion **34**, 1803 (1992).
8. B.A. Carreras, IEEE Trans. Plasma Sci. **25**, 1281 (1997).
9. R.J. Taylor, in *Proc. 11th Int. Conf. on Plasma Physics and Controlled Nuclear Fusion Research, Kyoto, 1986* (IAEA, Vienna, 1987) Vol. 1, p. 110.
10. P.H. Rebut, P.P. Lallia, Fusion Eng. Design **11**, 1 (1988).
11. Pulsator-team, Nuclear Fusion **25**, 1059 (1985).
12. F. Wagner, Ion energy balance in Pulsator, IPP Pulsator report III/52, Oct. 1979.
13. K. Lackner et al., Plasma Phys. Control. Fusion **31**, 1629 (1989).
14. S. Morita et al., in *Proc. 14th Int. Conf. on Plasma Physics and Controlled Nuclear Fusion Research, Würzburg, 1992* (IAEA, Vienna, 1993) Vol. 2, p. 515.
15. E.A. Lazarus et al., J. Nucl. Mater. **121**, 61 (1984).
16. Yu.V. Esipchuk et al., Plasma Phys. Control. Fusion **28**, 1253 (1986).
17. J.D. Strachan et al., Phys. Rev. Lett. **58**, 1004 (1987).
18. A.M. Messian et al., Nuclear Fusion **34**, 825 (1994).
19. R.R. Weynants et al., Nuclear Fusion **39**, 1637 (1999).
20. M. Greenwald, et al., Phys. Rev. Lett. **53**, 352 (1984).
21. JET Team, in *Proc. 12th Int. Conf. on Plasma Physics and Controlled Nuclear Fusion Research, Nice, 1988* (IAEA, Vienna, 1989) Vol. 1, p. 215.
22. K. Ida et al., Plasma Phys. Control. Fusion **38**, 1433 (1996).
23. ASDEX team, Nuclear Fusion **29**, 1959 (1989); written on the basis of the IPP internal report by F. Wagner "Confinement studies on ASDEX", IPP III/131, Feb. 1988.
24. K.H. Burrell et al., Plasma Phys. Control. Fusion **34**, 1859 (1992).
25. F. Wagner, Plasma Phys. Control. Fusion **49**, B1 (2007).

[21] For Bohm transport: see reference [1].

26. F. Wagner et al., Phys. Rev. Lett. **49**, 1408 (1982).
27. F. Wagner et al., Variation of the particle confinement during neutral injection into ASDEX divertor plasmas, IPP III/78, June 1982.
28. K. Itoh, Plasma Phys. Control. Fusion **36**, A307 (1994).
29. F. Ryter et al., Plasma Phys. Control. Fusion **40**, 725 (1998).
30. M. Keilhacker et al., Plasma Phys. Control. Fusion **26**, 49 (1984).
31. F. Wagner et al., First results from neutral beam heating of diverted ASDEX discharges, *Proceedings of the 3rd Joint Grenoble–Varenna International Symposium*, Centre d'Études Nucléaires de Grenoble–France, 22–26 March 1982, pp. 35-48.
32. F. Wagner et al., in *Proc. 9th Int. Conf. on Plasma Physics and Controlled Nuclear Fusion Research, Baltimore, 1982* (IAEA, Vienna, 1983), Vol. 1, p. 43.
33. S.M. Kaye et al., J. Nucl. Mater. **121**, 115 (1984).
34. M. Nagami et al., Nuclear Fusion **24**, 183 (1984).
35. A. Tanga et al., in *Proc. 11th Int. Conf. on Plasma Physics and Controlled Nuclear Fusion Research, Kyoto, 1986* (IAEA, Vienna, 1987), Vol. 1, p. 65.
36. D.A. Gates et al., Phys. Plasmas **5**, 1775 (1998).
37. A. Sykes et al., Phys. Rev. Lett. **84**, 495 (2000).
38. V. Erckmann et al., Phys. Rev. Lett. **70**, 2086 (1993).
39. K. Toi, et al., in *Proc. 14th Int. Conf. on Plasma Physics and Controlled Nuclear Fusion Research, Würzburg, 1992* (IAEA, Vienna, 1993), Vol. 2, p. 461.
40. A. Fujisawa, Plasma Phys. Control. Fusion **45**, R1 (2003).
41. F. Wagner, Plasma Phys. Control. Fusion **48**, 217 (2006).
42. J.W. Connor, H.R. Wilson, Plasma Phys. Control. Fusion **42**, R1 (2000).
43. D.J. Ward, Plasma Phys. Control. Fusion **38**, 1201 (1996).
44. F. Wagner et al., Phys. Rev. Lett. **53**, 1453 (1984).
45. H. Zohm, Plasma Phys. Control. Fusion **38**, 105 (1996).
46. J.W. Connor et al., Phys. Plasmas **5**, 2687 (1998).
47. K.H. Burrell et al., Plasma Phys. Control. Fusion **31**, 1649 (1989).
48. K. Itoh, S.-I. Itoh, A. Fukuyama, *Transport and Structural Formation in Plasmas* (IOP Publishing, Bristol, 1999).
49. U. Stroth et al., Plasma Phys. Control. Fusion **53**, 024006 (2011). A tutorial on the electric field and its role is part of the paper.
50. H.E. Mynick, W.N.G. Hitchon, Nuclear Fusion **23**, 1053 (1983).
51. H. Idei et al., Phys. Rev. Lett. **71**, 2220 (1993).
52. V. Erckmann, et al., in *Proc. 16th Int. Conf. on Plasma Physics and Controlled Nuclear Fusion Research, Montreal, 1996* (IAEA, Vienna, 1997), Vol. 2, p. 119.
53. K. Itoh, S.-I. Itoh, Plasma Phys. Control. Fusion **38**, 1 (1996).
54. S.-I. Itoh, K. Itoh, Phys. Rev. Lett. **60**, 2276 (1988).
55. K.C. Shaing, E.C. Crume, Phys. Rev. Lett. **63**, 2369 (1989).
56. K.H. Burrell, Phys. Plasmas **4**, 1499 (1997), and references therein.
57. R.J. Groebner, et al., Phys. Rev. Lett. **64**, 3015 (1990).
58. E.J. Doyle et al., Phys. Fluids B **3**, 2300 (1991).
59. R.A. Moyer et al., Phys. Plasmas **2**, 2397 (1995).
60. K.H. Burrell, Phys. Plasmas **6**, 4418 (1999).
61. W. Herrmann, ASDEX Upgrade Team, Phys. Rev. Lett. **75**, 4401 (1995).
62. H. Biglari, P.H. Diamond, P.W. Terry, Phys. Fluids **B2**, 1 (1990).
63. B. Lehnert, Phys. Fluids **9**, 1367 (1966).
64. Ch. P. Ritz et al., Phys. Rev. Lett. **65**, 2543 (1990).
65. P.H. Diamond, Y.B. Kim, Phys. Fluids **B3**, 1626 (1991).
66. A.F. Thompson, W.R. Young, J. Atmospheric Sci. **64**, 3214 (2007).
67. S. Coda et al., Phys. Rev. Lett. **86**, 4835 (2001).
68. M. Jakubowski et al., Phys. Rev. Lett. **89**, 265003 (2002).
69. A. Fujisawa et al., Phys. Rev. Lett. **93**, 165002 (2004).
70. P.H. Diamond, S.-I. Itoh, K. Itoh, T.S. Hahm, Plasma Phys. Control. Fusion **47**, R35 (2005).
71. C. Holland et al., Phys. Rev. Lett. **96**, 195002 (2006).

72. M. Shats, W. Solomon, Phys. Rev. Lett. **88**, 045001 (2002).
73. E. Sánchez et al., Contributions to Plasma Physics **38**, 93 (1998).
74. P. Manz et al., Phys. Rev. Lett. **103**, 165004 (2009).
75. A. Fujisawa et al., Plasma Phys. Control. Fusion **48**, S 205 (2006).
76. M.G. Shats et al., Phys. Rev. E **71**, 046409 (2005).
77. Y.H. Xu et al., Phys. Rev. Lett. **84**, 3867 (2000).
78. R.A. Moyer et al., Phys. Rev. Lett. **87**, 135001 (2001).
79. K.H. Burrell, Plasma Phys. Control. Fusion **48**, A347 (2006).
80. A. Hasegawa, M. Wakatani, Phys. Rev. Lett. **59**, 1581 (1987).
81. J. Schirmer et al., Nuclear Fusion **46**, S780 (2006).
82. R.R. Weynants, G. Van Oost, Plasma Phys. Control. Fusion **35**, B117 (1993).
83. Y. Miura et al., in *Proc. 16th Int. Conf. on Plasma Physics and Controlled Nuclear Fusion Research, Montreal, 1996* (IAEA, Vienna, 1997), Vol. 1, p. 167.
84. R.J. Taylor et al., Phys. Rev. Lett. **63**, 2365 (1989).
85. R.R. Weynants et al., Nuclear Fusion **32**, 837 (1992).
86. V. Rozhanski, M. Tendler, *Reviews of Plasma Physics* (Consultants Bureau, N.Y. & London, 1996), Vol. 18, p. 147
87. T. Shoij et al., in *Proc. 14th Int. Conf. on Plasma Physics and Controlled Nuclear Fusion Research, Würzburg, 1992* (IAEA, Vienna, 1993) Vol. 1, p. 323.
88. T. Estrada et al., Europhys. Lett. **92**, 35001 (2010).
89. P.H. Diamond et al., Phys. Rev. Lett. **72**, 2565 (1994).
90. E.J. Kim, P.H. Diamond Phys. Rev. Lett. **90**, 185006 (2003).
91. P. Manz et al., Phys. Rev. E **82**, 056403 (2010).
92. G.D. Conway et al., Phys. Rev. Lett. **106**, 065001 (2011).
93. L. Schmitz et al. Phys. Rev. Lett. **108**, 155002 (2012), and references therein.
94. E.J. Doyle et al., in *Proc. 14th Int. Conf. on Plasma Physics and Controlled Nuclear Fusion Research, Würzburg, 1992* (IAEA, Vienna, 1993), Vol. 1, p. 235.
95. Y. Andrew et al., Europhys. Lett. **83**, 15003 (2008).
96. G.L. Jackson et al., Phys. Rev. Lett. **67**, 3089 (1991).
97. O. Gruber et al., Phys. Rev. Lett. **74**, 4127 (1995).
98. O. Gruber et al., Nuclear Fusion **49**, 115014 (2009).
99. R.C. Wolf et al., Plasma Phys. Control. Fusion **41**, B93 (1999).
100. Y. Takase et al., in *Proc. 16th Int. Conf. on Plasma Physics and Controlled Nuclear Fusion Research, Montreal, 1996* (IAEA, Vienna, 1997), Vol. 1, p. 475.
101. K.H. Burrell et al., Bull. Am. Phys. Soc. **44**, 127 (1999).
102. F. Ryter et al., Plasma Phys. Control. Fusion **40**, 725 (1998).
103. D.G. White et al., Nuclear Fusion **50**, 105005 (2010).
104. K. McCormick et al., Phys. Rev. Lett. **89**, 015001-1 (2002).
105. Y. Kamada, Plasma Phys. Control. Fusion **38**, 1173 (1996).
106. R.C. Wolf, Plasma Phys. Control. Fusion **45**, R1 (2003).
107. J.W. Connor et al., Nuclear Fusion **44**, R1 (2004).
108. G.L. Schmidt et al., in *Proc. 12th Int. Conf. on Plasma Physics and Controlled Nuclear Fusion Research, Nice, 1988* (IAEA, Vienna, 1989), Vol. 1, p. 215.
109. C. Kessel et al., Phys. Rev. Lett. **72**, 1212 (1994).
110. K. Lackner et al., Plasma Phys. Control. Fusion **42**, B37 (2000).
111. Z.A. Pietrzyk et al., Phys. Rev. Lett. **86**, 1530 (2001).
112. Y. Koide et al., Phys. Rev. Lett. **72**, 3662 (1994).
113. F.M. Levinton et al., Phys. Rev. Lett. **75**, 4417 (1995).
114. E.J. Strait et al., Phys. Rev. Lett. **75**, 4421 (1995).
115. C. Gormezano and JET Team, in *Proc. 16th Int. Conf. on Plasma Physics and Controlled Nuclear Fusion Research, Montreal, 1996* (IAEA, Vienna, 1997), Vol. 1, p. 487.
116. Equipe Tore Supra, in *Proc. 15th Int. Conf. on Plasma Physics and Controlled Nuclear Fusion Research, Seville, 1994* (IAEA, Vienna, 1995), Vol. 1, p. 105.
117. T. Fujita et al., Phys. Rev. Lett. **78**, 2377 (1997) [Erratum: Phys. Rev. Lett. **78**, 4529 (1997)].

118. E.J. Synakowski et al., Phys. Rev. Lett. **78**, 2972 (1997).
119. Y. Koide et al., Phys. Plasmas **4**, 1623 (1997).
120. U. Stroth et al., Phys. Rev. Lett. **86**, 5910 (2001).
121. B.J.D. Tubbing et al., Nuclear Fusion **31**, 839 (1991).
122. E.A. Lazarus et al., Phys. Rev. Lett. **77**, 2714 (1996).
123. T.S. Taylor et al., *Controlled Fusion and Plasma Physics (Proc. 21st Eur. Conf. Montpellier, 1994)* (European Physical Society, Geneva, 1994), Vol. 18B, Part 1, p. 403.
124. M. Hugon et al., Nuclear Fusion **32**, 33 (1992).
125. D.R. Ernst et al., Phys. Rev. Lett. **81**, 2454 (1998).
126. A. Fukuyama et al., Plasma Phys. Control. Fusion **36**, A159 (1995).
127. T.S. Taylor et al., in *Proc. 17th Int. Conf. on Plasma Physics and Controlled Nuclear Fusion Research, Yokahama, 1998* (IAEA, Vienna, 1999), Vol. 1, p. 49.
128. Y. Hamada et al., Plasma Phys. Control. Fusion **48**, S177 (2006).
129. Y. Nagashima et al., Plasma Phys. Control. Fusion **48**, S1 (2006).
130. P.W. Terry, Rev. Mod. Phys. **72**, 109 (2000).
131. P.H. Diamond et al., in *Proc. 14th Int. Conf. on Plasma Physics and Controlled Nuclear Fusion Research, Würzburg, 1992* (IAEA, Vienna, 1993), Vol. 2, p. 97.
132. *Reviews of Plasma Physics*, edited by M.A. Leontovish (Consultants Bureau, New York, 1970), Vol. 5, p. 249.